BIOLOGIA PLANTARUM 55 (3): 469-478, 2010

Microsporogenesis and pollen formation in cassava

C. WANG[1]*, Z. LENTINI[2]*, E. TABARES[3], M. QUINTERO[3], H. CEBALLOS[3,4]**, B. DEDICOVA[3], C. SAUTTER[5], C. OLAYA[3] and P. ZHANG[6]

South China Botanical Garden, Chinese Academy of Sciences, Xingke Road 723, Guangzhou 510650, China[1]
Universidad ICESI, Calle 18 No. 122-135, Cali, Colombia [2]
International Center for Tropical Agriculture, Km17, Recta Cali-Palmira, AA 6713 Cali, Colombia[3]
Universidad Nacional de Colombia. Palmira Campus. Carrera 32, Chapinero. Palmira, Valle del Cauca, Colombia[4]
Institute of Plant Sciences, Swiss Federal Institute of Technology, CH-8092, Zurich, Switzerland[5]
Shanghai Institutes for Biological Sciences, Chinese Academy of Sciences, Shanghai 200032, China[6]

Abstract

This article describes the complete microsporogenesis and pollen formation in cassava (*Manihot esculenta* Crantz) at the various developmental stages (pollen mother cell, meiosis, tetrads, early free spore, mid uninucleate, late uninucleate, binucleate and mature pollen grain). Light microscopy, transmission electron microscopy and confocal laser scanning microscopy were used for the study. Floral bud size and other inflorescence characteristics were correlated with specific stages of the microspore development. This association allows a rapid selection of floral buds with similar microspore developmental stages, useful when a large number of homogeneous cells are needed for analysis and for *in vitro* induction of androgenesis. This article also compares methods for digestion the exine wall in microspores.

Additional key words: CLSM, FISH, exine digestion, *Manihot esculenta*, ultrastructure.

Introduction

The life cycle of flowering plants involves the alternations of a diploid sporophytic and haploid gametophytic phase (Li *et al*. 2009, Taskin *et al*. 2009). Microsporogenesis occurs at the end of the sporophytic phase and undergoes a clearly defined cell division program resulting in a gametophyte (pollen grain) comprising the generative and vegetative cells. The generative cell divides giving rise to two sperm cells (McCormick 2004). The developmental events of microsporogenesis and pollen formation are exquisitely timed and choreographed, occurring in a precise chronological order that correlates with the floral bud size (Koltunow *et al.* 1990, Scott *et al.* 1991). Efforts have frequently been made to describe microsporogenesis and pollen formation from the cytological, molecular and genetic perspectives largely in model plant species (Goldberg *et al.* 1993, McCormick 2004, Scott *et al.* 2004, Chen *et al*. 2005, Blackmore *et al.* 2007). However, these processes are poorly understood in other plant species such as cassava. Cassava is a perennial shrub, vegetatively propagated and grown throughout lowland tropics. The heterozygous nature of the progenitors complicates traditional breeding as well as genetic and molecular studies. Production of homozygous lines *via* doubled-haploids through the *in vitro* culture of microspores (androgenesis) would facilitate and accelerate the development of advanced germplasm and genetic analysis (Ceballos *et al.* 2004, 2007). The

Received 10 December 2009, *accepted* 17 March 2010.
Abbreviations: CLSM - confocal laser scanning microscope; FISH - fluorescent *in situ* hybridization; DAPI - 4'-6-diamidino-2-phenylindole; PMC - pollen mother cell; EFS - early free spore; T - tapetum; M - middle layer; EN - endothecium; E - anther epidermis.
Acknowledgements: The excellent technical support on microscopy provided by José Arroyave is hereby recognized. Valuable comments by Dr. Stephen Blackmore on an earlier version of this manuscript have been incorporated. This work was supported through the grant project No. 2003 FS 121 and No. 2006 FS 062 by The Rockefeller Foundation, NY, USA, and Research Fellow Partnership Programme (RFPP), Switzerland.
* Previously at International Center for Tropical Agriculture
** Corresponding author; fax: (+57) 2 4450073, e-mail: b.dedicova@cgiar.org

induction of androgenesis requires the culture of microspores at specific developmental stages. Thus the understanding of microsporogenesis and pollen formation in cassava is an important pre-requisite for the development and application of this technology.

This article provides a comprehensive description of the *in vivo* microsporogenesis and pollen formation processes in cassava, the identification and association of microspore developmental stages with specific inflorescence and floral bud characteristics, as well as the application for the development of protocols for *in vitro* production of doubled haploids.

Materials and methods

Cassava (*Manihot esculenta* Crantz) clones, HMC-1 and TAI-8 were planted in the field at Corpoica Experimental Station in Palmira, Colombia. Vegetative cuttings were planted and after sprouting, conventional cultural practices were applied during the entire growing cycle through maturity (Ospina and Ceballos 2002). Inflorescences were collected at 08:00 - 10:00 from healthy and vigorous plants with profuse flowering, and of similar morphology and developmental stage. After collection floral buds were immediately stored in a polystyrene box with refrigerant gel (*Pelton Shepherd Industries*, Stockton, CA**,** USA) to avoid physiological deterioration during transportation.

For the analysis of mother pollen cells, flower buds were fixed in Carnoy solution for 24 h and then preserved in ethanol (75 %). Anthers were extracted from flower buds, squashed in aceto-carmine (2 %) for 5 min and then analyzed with the *Leica* microscope (*Leica Microsystems*, Heidelberg, Germany). Microphotographs were taken using a photo automat camera (model *MPS45*, Heerbrugg, Switzerland). The developing exine structure of mature tetrads was photographed using contrast phase optics with a *Leica* microscope (*Laborlux*, Heidelberg, Germany).

Additionally, intact fresh buds and anthers were first fixed in 2.5 % glutaraldehyde (in 0.1 M phosphate buffer, pH 7.2) for 24 h at 4 °C and post-fixed in aqueous osmium tetroxide (1 %) during 1 h. Samples were then washed three times with distilled water and dehydrated in a ethanol series (25, 50 and 75 %). Specimens were immersed in 2 % uranyl acetate (in 75 % ethanol) for 12 h at room temperature, followed by immersion 1 × in 90 % ethanol and 3 × in 100 % ethanol. Samples were rinsed with pure acetone for 20 min (three times) and then gradually embedded in acetone-Spurr epoxy resin (1:1). Anthers were later infiltrated in pure Spurr epoxy resin for 1 h. Finally, samples were polymerized at 60 °C for 16 h. Embedded anthers were sectioned on an ultra microtome (*MT 6000*, *Sorvall Instruments*, DuPont, Delaware, USA) for semi-thin or ultra-thin sections. The semi-thin sections were stained with toluidine blue-O and analyzed with the *Leica* microscope. The ultra-thin samples were cut with a diamond knife at 60 nm, collected in copper grids and stained with uranyl acetate and lead citrate following Reynolds (1963) procedure. The ultra-thin sections were examined with a transmission electron microscope *Jeol TM1010* (Tokyo, Japan). The images were captured and analyzed using *AnalySIS 3.0* software (*Soft Imaging* System, Münster, Germany).

In addition to the light and electron microscopy evaluations, samples were also analyzed under a fluorescence confocal scanning microscope (*Leica TCS SP2 Confocal*). Because of the exine thickness and auto-fluorescence, the anthers were first fixed in a FAA (ethanol: glacial acetic acid: formalin: H_2O; 50: 5: 10: 35) solution for at least 24 h and then treated with 10 % sodium hypochlorite for 2 min to digest the exine. Microspores with partially digested exines were washed three times in deionized distilled water and stained with 0.05 mg cm^{-3} of acridine orange (AO). The images were captured by a *Leica Confocal* software and processed using *Imaris 3D* software version *4.2.0* (*Bitplane AG*, Zurich, Switzerland).

In order to use effectively confocal laser scanning microscope (CLSM), it was necessary first to treat the microspores to degrade exine wall. Different alternatives of the standard procedure reported in the literature (Rowley *et al.* 1999) based on $KMnO_4$ were evaluated. Microspores were treated with 0.5, 1.0, 2.0, 4.0, 8.0 and 16.0 % $KMnO_4$ solutions for time periods ranging from 1 min up to 24 h. Microspores were also treated with 10 % NaOCl to remove the exine and eliminate the source of the microspore auto-fluorescence, therefore allowing the penetration of the laser beam across the microspore and use of the corresponding fluorescent staining.

Developed pollen grains were fixed in a solution of 96 % ethanol : glacial acetic acid (3:1; v/v) for 10 - 15 min, washed with 70 % ethanol centrifugation at 150 *g* for a 2 min and stained in 4'-6-diamidino-2-phenylindole (DAPI; *Partec*, Münster, Germany) and observed under the fluorescent microscope.

For light microscopy analysis, about 200 pollen mother cells or tetrads (about 2000 microspores) from 10 - 20 male buds were processed at each specific bud size. For the electron microscopy studies, five male buds were processed for each size. CLSM and exine digestion analyses were based on microspores isolated from ten buds for each of the following sizes: 2.4, 2.5, 2.6 and 2.7 mm. Buds were taken from different plants**.**

Results and discussion

The combination of different techniques (standard aceto-carmine staining protocols using fresh anther squashes and light microscopy at pre-meiosis stage, fixed-sectioned samples for light and electron microscopy, and exine-digested microspores for CLSM at the post-meiosis stage) allowed identifying the complete microsporo-genesis process, step by step from the pollen mother cell stage to mature pollen grain.

Only 16.0 % $KMnO_4$ solutions could degrade the exine wall after 24 h of treatment, but success frequency was low and cells usually had deteriorated and lost viability. Since part of this work aimed at inducing cell divisions within the microspore for the production of doubled-haploids, this technique was no longer pursed. Alternatively, the use of NaOCl proved to be both useful in degrading exine wall and preserving the viability of a proportion of the microspores for future manipulation (provided that additional measures were taken).

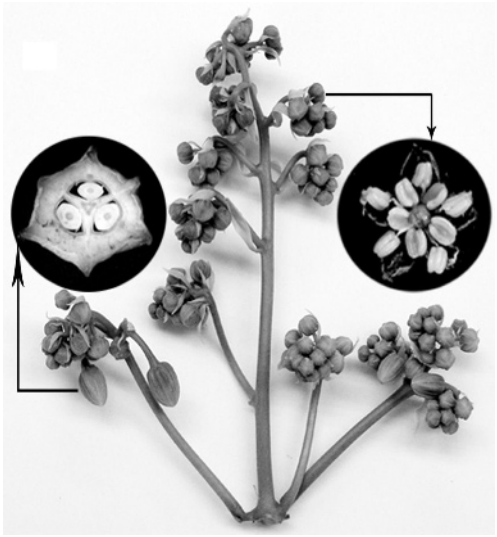

Fig. 1. Cassava inflorescence. *Left* - traversal section of the ovary; *right* - dissected male floral bud.

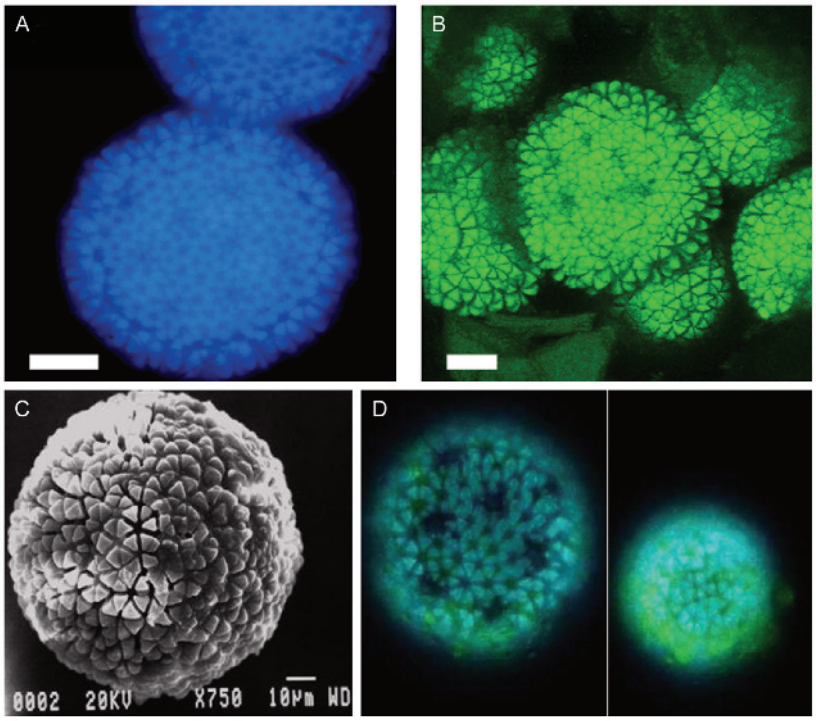

Fig. 2. Fluorescent images of microspores: *A* - auto-fluorescence from untreated freshly isolated microspores examined at the same wavelength and parameters as those used for DAPI detection, *bar* = 20 µm; *B* - 3-dimensional reconstruction of a microspore using CLSM autofluorescence signal, *bar* = 20 µm; *C* - mature cassava pollen, photographed by scanning electron microscope, showing the reticulated exine pattern; *D* - dimorphism in cassava pollen determined using epifluorescence microscope.

female and male flowers on the same plant. Inflorescences are generally terminal and formed at the insertion point of the reproductive branching (Alves 2002). Typically, two female flowers (3-ovule ovary) are located at each basal branch of the inflorescence. The rest of the inflorescence branches contain male flowers, which significantly out-number female flowers (50 to 200 male flowers per inflorescence). The calyx of male flowers is campanulated, imbricate-lobes 5, petals 0, stamens 10 (Fig. 1). The average diameter of cassava

uninucleate microspore is 50 μm. Mature pollen grains, on the other hand, average 160 μm in size. Each cassava anther produces between 100 and 200 microspores. The size of cassava microspores and pollen grains are considerably larger than those from other cultivated flowering plants such as cereals (Hrabina *et al.* 2008) or soybean (Koti *et al.* 2004). The number of pollen grains within each anther is considerably lower than those found in cereals or soybean (1 000 and 500 microspores, respectively). Pollination of *Manihot* species is mostly made by insects particularly honeybees (Da Silva *et al.* 2001), whereas in the case of cereals, it is by wind. This explains the differences in the amount of pollen produced and their size.

Observations under light and fluorescence microscope indicated that a thick-opaque, well-ornamented and auto-fluorescent exine wall develops in cassava young microspores, immediately after their release from tetrads (Fig. 2). Immature exine or primexine in the microspores released under pressure from the callose wall, showed a distinctive reticulate pattern. The exine thickness at the late uninucleate stage, determined by electron microscopy, ranges from 10 to 15 μm (Fig. 3*s*) and was relatively uniform around the microspore. The thickness and auto-fluorescence of the exine hinder the use of conventional methods to stain the nucleus such as aceto-carmine, and DNA specific fluorochrome like DAPI or cell viability indicator fluorochrome such as fluorocein diacetate (FDA). These features of the exine also prevent the easy analysis to determine the microspore stage of development. In order to circumvent these technical bottlenecks, fixed and semi-thin sections stained samples were used for light microscopy. To complement the light microscopy observations, electron microscopy of the ultra-thin sections and CLSM analyses, were also conducted.

Seven main phases were identified throughout cassava microsporogenesis and pollen formation, which seems to follow exactly the same pattern revealed in other eudicots as reviewed by McCormick (2004) and Scott *et al.* (2004).

PMC stage: Squash of anthers from floral buds of 1.8 to 2.0 mm in diameter easily releases pollen mother cells. This has been regarded as a common feature of pollen mother cells at the early stages of development in several different species (Esau 1977) and has been presumed to be due to the presence of cytoplasmic channels between adjacent PMCs (Owen and Makaroff 1995, Boavida *et al.* 2005). This kind of cytoplasmic continuum between meiocytes (pollen mother cells) may contribute to an effective synchronization during microsporogenesis, by allowing exchange of molecules and ions (Heslop-Harrison 1966, Mascarenhas 1975). A large, centrally located, prominent nucleus stained with aceto carmine is clearly distinguished in each PMC as well as a distinct callose wall (Fig. 3*a*). PMCs are enclosed in the locular matrix and typically surrounded by four layers of cells: the tapetum (T), the middle layer (M), the endothecium (EN) and the anther epidermis (E) (Fig. 3*b*-*c*). This structure is similar to that described in *Arabidopsis* (Owen and Makaroff 1995). Tapetal cells are about 20 % the size of PMCs (Fig. 3*b*). The densely stained tapetal cells are about four times larger than those of the other three surrounding layers of cells, which are abutted tightly to the tapetum. At this stage of development, both large vacuoles and multi-nuclei were present in the tapetal cells with a well-defined cell wall (Fig. 3*b*-*c*). Cells in the middle layer, the endothecium, and epidermis were lightly stained by toluidine blue (Fig. 3*b*).

Meiosis occurs at the PMCs stage. Our results corroborate earlier reports indicating the presence of 36 small and very similar chromosomes, and 18 bivalent pairing at meiosis in cassava (Jennings 1963, De Carvalho *et al.* 2002). For the prophase I, leptotene, pachytene and diakinesis were identified. At the zygotene stage, due to the chromatin condensation chromosomes become visible as extended thread-like structures and a big nucleoli is clearly visible (Fig. 3*d*). Chromosomes are fully synapsed and well expanded at the pachytene stage (Fig. 3*e*). Considering that the cells at this stage are about 90 μm in diameter and the chromatin is well spread in the cell, this stage could be a good target for cytogenetic studies using fluorescent *in situ* hybridization (FISH). At diakinesis, the chromosomes start showing a higher degree of condensation (Fig. 3*f*) in preparation for metaphase I (Fig. 3*g*). During metaphase I, eighteen homologous chromosomes paired up on the metaphase plate. All chromosomes are similar in their degree of high condensation and relatively uniform in size. During anaphase I, the homologous chromosomes separated, allowing for chromosomal counting (Fig. 3*h*), and move towards opposite poles driven by the spindle apparatus (Fig. 3*i*). It is interesting to note that the chromosome segregation tended to occur in alternate almost perpendicular planes in adjacent cells (Fig. 3*i*).

After anaphase I, the PMCs are unconnected and easily separated. At prophase II, re-condensed chromosomes are clearly displayed at both cell poles (Fig. 3*j*). The following anaphase II stage is distinguished in each cell (Fig. 3*k*). Two independent chromosome segregation events, controlled by two sets of spindle apparatuses, are clearly distinguishable. At the end of telophase II a simultaneous cytokinesis occur giving rise to tetrads as described below.

Tetrad stage: Tetrads arrange in a tetrahedral configuration, characterized by having one of the four cells in one plane opposed to the other three cells (Fig. 3*l*). The arrangement of tetrads may change at later stages of their development (Fig. 3*m*). Similar processes have been described for other plant species (Khan *et al.*

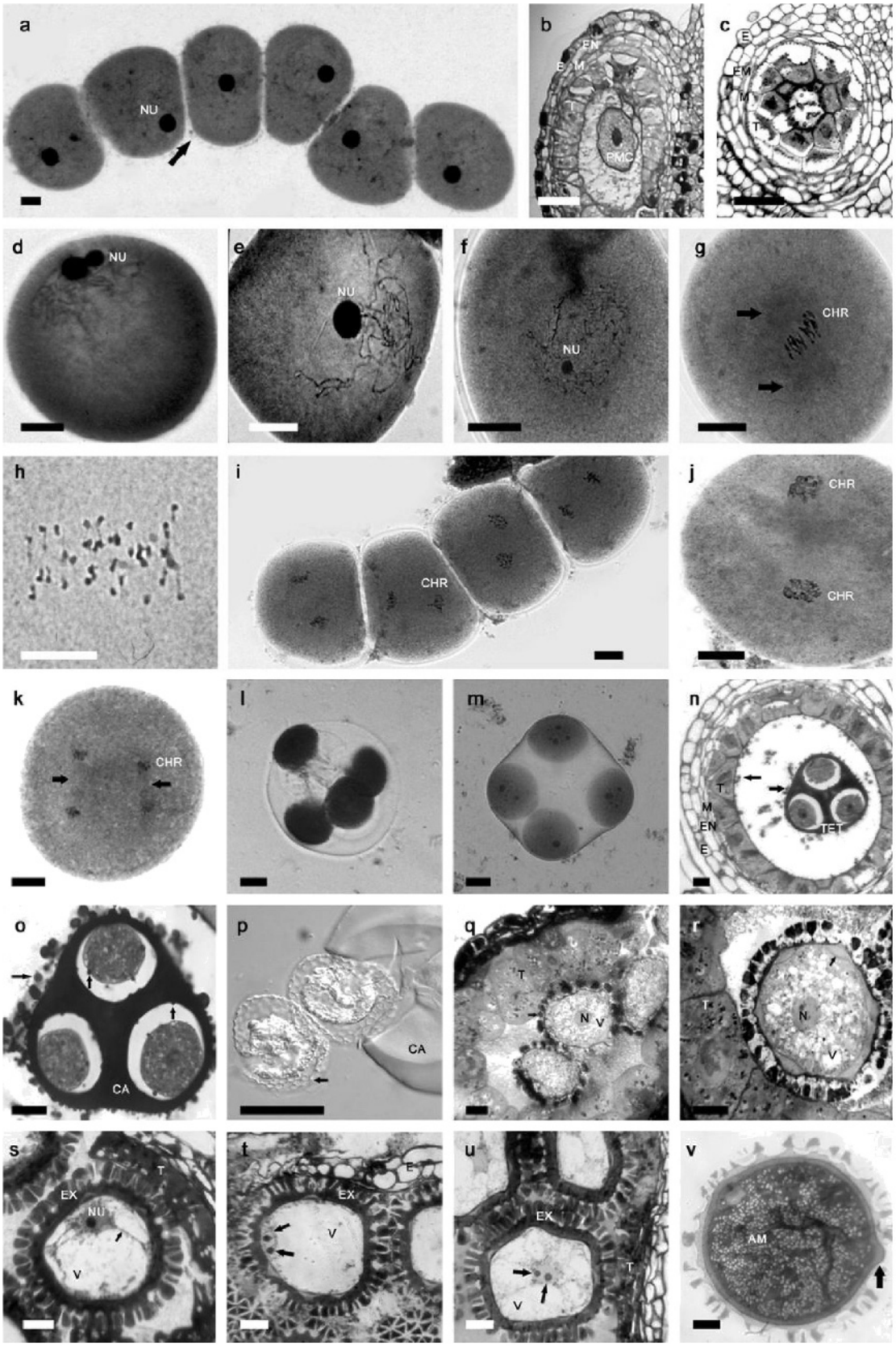
a
NU
b
EN
E
M
T
PMC
c
E
EM
M
T
d
NU
e
NU
f
NU
g
CHR
h
i
CHR
j
CHR
CHR
k
CHR
l
m
n
T
M
EN
E
TET
o
CA
p
CA
q
T
N
V
r
T
N
V
s
T
EX
NU
V
t
E
EX
V
u
EX
T
V
v
AM

Fig. 3. Microsporogenesis and pollen formation images using light microscopy: *a* - pollen mother cells (PMCs) released from anther squash showing a large nucleolus (NU) and negatively stained callose wall (*arrow*); *b* - longitudinal section of a single locule showing a PMC and four layers of cells surrounding it; *c* - Transversal section of a single locule showing a PMC developing into microsporocyte in the center surrounded by tapetal cells [tapetum (T), the middle layer (M), the endothecium (EN) and the epidermis (E)], *bar* = 100 μm; *d* - zygotene stage of meiosis; *e* - pachytene stage of meiosis; *f* - diakinesis stage of meiosis; *g* - metaphase I, note that the chromosomes (CHR) are aligned in the middle of the cell; *h* - early anaphase I showing the well spread 18 bivalents, *bar* = 10 μm; *i* - anaphase I, note that the different direction of equatorial planes between any two adjacent PMCs; *j* - prophase II shows the two sets of re-condensed chromosomes; *k* - anaphase II, note the four chromosome sets and the two sets of spindle apparatuses (*arrow*); *l* - simultaneous cytokinesis showing tetrahedral arrangement; *m* - microsporocytes close to their release as free spores; *n* - transversal section through a tetrahedral tetrad (TET) showing the dark-stained globules (*arrow*); *o* - detail of the tetrad from *N* showing the distribution of the dark-stained globules (*arrow*) and callose wall (CA) very darkly stained; *p* - tetrad releasing free spores after slight hand squash showing the reticulum-like exine structure; *q* - EFS stage, note the swollen tapetal cells (T), the widely spaced tectum (*arrow*) and small vacuoles (V); *r* - mid uninucleate stage, note the clearly identified aperture (*arrow*); *s* - late uninucleate stage showing degraded tapetum (T), well developed exine (EX), cytoplasmic strand (*arrow*) and large vacuoles (V); *t* - binucleate stage showing the two nucleoli (*arrows*) and one big vacuole (V), note that the microspore is pressed against the epidermis (E) and the tapetum has disappeared in this section; *u* - binucleate stage in clone MTAI-8; - mature pollen grain showing large number of amyloplasts (AM), and the bulging aperture (*arrow*). *a* and *d* to *m* are stained with acetocarmine, *p* without staining, unless otherwise specify samples stained with toluidine blue O. Unless specified, *bar* = 20 μm.

1991, De Souza and Pereira 2000). A thick layer of callose wall, darkly stained by toluidine blue, coated the whole tetrad and separated the individual microspores. Primexine and procolumellae formation was observed in tetrads extracted from flower buds ranging from 2.0 to 2.2 mm in size. In the mature tetrads, the plasmalemma was pulled away from the callose wall leaving a space between them (Fig. 3*n*-*o*), allowing some darkly stained globules to be visible on the inner side of callose wall and outer side of plasmalemma. This kind of globules is also found in the inner side of tapetum and the locular matrix, but not in the space between the plasmalemma and callose wall (Fig. 3*n*-*o*). At this stage, except for the fact that most of the tapetal cells hold two distinct nuclei, all other characteristics of tapetal cells are similar to those at the PMCs stage (Fig. 3*b*,*n*). All tetrads from anthers within the same floral bud appear to be at the same developmental stage (data not shown) and characterized sometimes by clearly stained central nucleus and the absence of vacuoles (Fig. 3*n*-*o*).

Early free spore (EFS) stage: The callose wall breaks down and the four individual microspores are released from each tetrad. At this stage the intine is clearly visible and is surrounding the plasmalemma. Intine is thick in the aperture region and endexine appears as a thin layer that will become more noticeable at later stages. Ectexine appears as an electron dense layer with a thin foot layer and collumelae. On top of the collumelae the tectum becomes visible as pyramidal-shaped sculpture elements (Fig. 3*r*). The exine looks like a reticulum-loose structure (Fig. 3*q*), which might be used as a skeleton guiding further deposition of sporopollenin. This distinctive surface pattern observed in cassava pollen is called "crotonoid" patterning (Berry *et al.* 2005) and our results are probably the first describing early pollen development in a species with that pattern. Interestingly this means that much of the thickness of the exine is added during the free microspore stage – presumably by incorporation of sporopollenin from the tapetum. It is also interesting to note that first this pattern is established as a reticulate pattern and then the crotonoid tectum becomes thicker later in development (S. Blackmore, personal communication).

During this stage, dark sculptural particles are deposited on the tectum. These particles are widely spaced and absent in the aperture region, which becomes detectable for the first time only at this stage (Fig. 3*q*). The tectum layer in the aperture region is thinner than in other areas (Fig. 3*q*). A large centralized nucleus is present at the EFS stage. The EFS showed a distorted appearance in the locular matrix and microspores are surrounded by swollen tapetal cells. The tapetal cells showed at this stage a more complex structure than before. Tapetal cells become thinner with completely degraded cell walls, and contain multiple small vacuoles. On the other hand, the middle layer cells are pressed against the swollen tapetum. This may be an indication that the tapetum is physiologically active. As the volume of tapetal cells and EFS increase, the locular matrix is largely compressed and the EFS filled most of the space in the locule. Many small vacuoles are dispersedly distributed in the EFS cytoplasm (Fig. 3*q*). Intact EFS, < 60 μm in diameter, are transparent. EFS are found in floral buds 2.2 - 2.4 mm in diameter.

Mid uninucleate stage: Microspores of floral buds from 2.4 to 2.5 mm in diameter contain a large nucleus and become round, indicating that the cell wall is more rigid. Six apertures are identified at this stage. Small, scattered vacuoles are replaced by dozens of larger vacuoles (Fig. 3*r*), and occupied more than 50 % of the overall cell volume. The cytoplasm of the tapetal cells is dense and the tapetum remained relatively unchanged compared with the EFS stage. The microspores gradually become opaque and the exine auto-fluoresces strongly from this stage on.

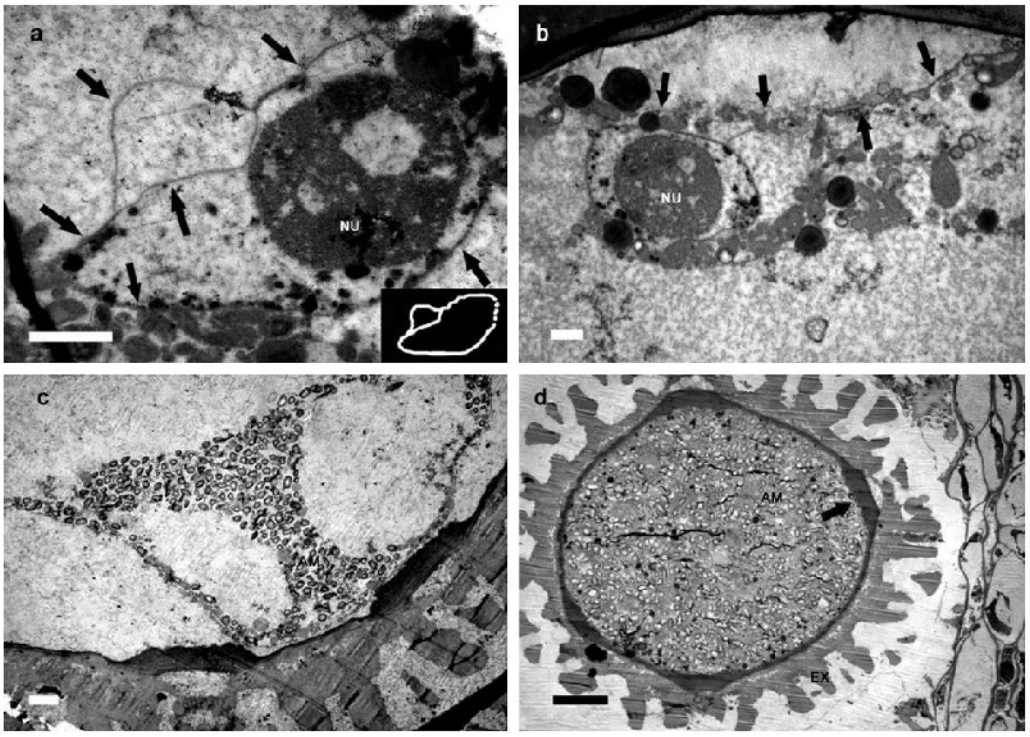

Fig. 4. Ultrastructure of microspores using transmission electron microscopy: *a* - binucleate stage, note the two sets of nuclear envelopes (*arrows*) are linked to each other; the large nucleolus (NU) of the vegetative nucleus (*right side*); *insert* represents the schematic view of the nuclear envelops, *bar* = 2 μm; *b* - binucleate stage showing the cell plate (*arrows*) around the generative cell is pressed against the intine layer, and the nuclear envelop enclosing the nucleolus (NU), *bar* = 2 μm; *c* - late binucleate stage showing the accumulation of amyloplasts, *bar* = 2 μm; *d* - mature pollen grain showing amyloplasts (AM) and the aperture (*arrow*), *bar* = 20 μm

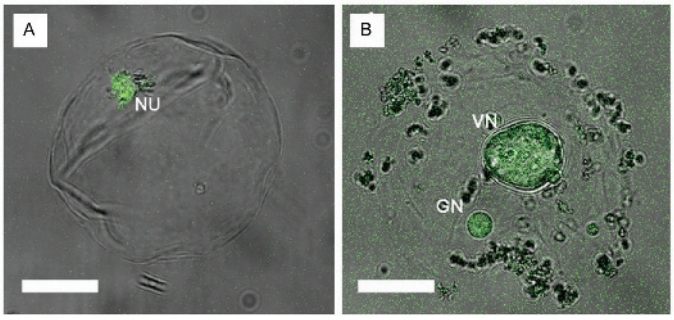

Fig. 5. Fluorescence image of microspores using CLSM: *A* - microspore at uninucleate stage using samples with fully digested exine and stained with acridine orange clearly showing the nucleus (NU); *B* - binucleate microspore using the same method as in *A* showing the large vegetative nucleus (VN) and the small generative nucleus (GN). *Bar* = 20 μm.

Late uninucleate stage: Microspores become highly vacuolated with fewer but larger vacuoles occupying more than 90 % of the cell volume. These vacuoles can be seen separated by cytoplasm strands (Fig. 3*s*). The cytoplasm is restricted to a side of the cell pushed towards a section of the periphery. In the ectexine, the foot layer, collumelae and tectum are well developed and are clearly visible. The pyramid-like sculptural elements of the tectum are arranged in a reticulate pattern. Six to seven of these elements are grouped together and arranged concentrically forming a hexagonal shape when viewed in cross-sections (Fig. 3*t*). No supratectal elements were observed. The exine pattern remains unchanged from this stage up until mature pollen grains develop. The tapetum is fragmented and begins to dissociate at this stage. Buds containing late uninucleate microspores are about 2.5 - 2.6 mm in the diameter. The uninucleate nature of these microspores was also confirmed by CLSM (Fig. 5*a*).

Binucleate stage: The interior structure of the microspore changes significantly as floral buds grow

slightly larger. The tapetum degraded almost completely (Fig. 3*t*). The degradation of the tapetum shows a strong association with the exine wall formation on the microspore surface, supporting the hypothesis that the tapetum plays a vital role in nourishing the microspores and the formation of exine (Koltunow *et al.* 1990, Mariani *et al.* 1990, Goldberg *et al.* 1993). Microspores remain highly vacuolated at this stage (Fig. 3*t*,*u*). The largely reduced cytoplasm contains two nucleoli densely stained with toluidine blue-O, each one belonging to different nucleus, as confirmed by electron microscopy (Fig. 4*a*) and by CLSM (Fig. 5*B*). Electron microscopy of step-wise serial cross microspore sections revealed two nuclear envelopes. One nuclear envelope contains one electron-dense large nucleolus belonging to the vegetative nucleus (Fig. 4*a*). The second envelope on the left side (Fig 4*a*) does not show the nucleolus, most likely belonging to the generative nucleus, which may be at a different plane section (Fig. 4*a*), and it is seen also in another section (Fig. 4*b*). Analysis with CLSM provides complementary evidence corroborating that these microspores contain two nuclei: a large vegetative nucleus and a smaller generative one (Fig. 5*B*). Until this stage of development there is no obvious accumulation of amyloplasts. Similar results are obtained when using floral buds of 2.6 - 2.8 mm in diameter of either HMC-1 or MTA-8 clones, suggesting a consistent pattern, which is independent of the clones where the buds are collected. This criterion, therefore, could be used to predict the approximate developmental stage of microspores in other cassava clones.

Mature pollen grain stage: Floral buds > 2.8 mm in diameter contain pollen grains rich in amyloplasts scattered through the cytoplasm (Figs. 3*v*, 4*c*-*d*). Vacuoles are absorbed and amyloplasts accumulate readily until almost the entire cell is filled with amyloplasts (Fig. 4*d*). The average diameter of cassava pollen grains is about 160 µm (based on a sample size of 100 microspores). Pollen type is monade. However, mature pollen dimorphism was commonly observed in different cassava genotypes analyzed (Fig. 2*b*,*d*) and has been already reported. Although their germinating capacity is not the same, both pollen sizes proved to be fertile (Halsey *et al.* 2008). The complete sporoderm and slightly bulged portion of the aperture are clearly identified (Figs. 3*v*, 4*d*). Intine could be differentiated from the endexine and it is clearly bulged in the aperture and the endexine showed a granular texture (Fig. 4*d*). At the right side of Fig. 4*d* vestiges of an orbicule can also be observed. Ectexine is electron-dense and is thicker than at the uninucleate stage (Fig. 3*r*). It remains unclear whether the mature pollen cells are bi-nucleate or tri-nucleate because the amyloplasts, together with other inclusions, greatly affected the identification of nuclei in these cells. The richly ornamented reticulated "crotonoid" pattern of the exine is discerned with CLSM and scanning electron microscope imaging (Fig. 2*b*-*c*). Floral buds of 6.0 mm in diameter contain mature pollen grains capable of pollination.

Relationship between bud size and microspore development: In this study, there is a good relationship between the stages of anther development and floral bud length as reported in other crops (Kasperbauer *et al.* 1979, Summers *et al.* 1992, Custodio *et al.* 2005) and with the mean length of the two largest petals in rapeseed (Tomasi *et al.* 1999). In soybean, the microspores of different cultivars can be at different developmental stages for a given bud-size group (Lauxen *et al.* 2003). This type of difference has also been observed in *Brassica napus* and *B. oleracea* (Wang, personal observation). In our study, anthers from the same bud size range produced microspores that were at a similar development stage, independent of the two clones from which they were collected. However, since flower size varies in different genotypes, validation of our conclusions based on a larger sample of genotypes is needed.

A strong relationship between bud size and their corresponding microspore developmental found in cassava is useful for a rapid isolation of large and homogeneous samples of microspores at similar developmental stage. Two main bottlenecks have been identified for the development of an efficient protocol for androgenesis induction in cassava isolated microspores. The first bottleneck is that cassava floral buds yield a low amount of microspores (1000 - 2000 microspores per bud). However, microspore densities typically used for androgenesis range from 10^4 to 10^5 cells cm^{-3} medium (Fan *et al.* 1988, Huang *et al.* 1990, Kernan *et al.* 2006). If similar densities are to be used in cassava, at least hundreds of buds of homogeneous size are required to obtain a sample of microspores for culture.

The second bottleneck is the thick-opaque and autofluorescent-bearing exine wall, which jeopardized early efforts towards determination of nucleus number and microspore stage of development. For androgenesis induction, it is important to determine the optimal microspore stage of development (most responsive to division induction *in vitro),* and subsequent monitoring of the cell division using specific standard and fluorescent staining techniques such as aceto carmine (Kindiger and Beckett 1985), DAPI (Barinova *et al*. 2002), fluorescein diacetate (Widholm 1972) or propidium iodide (Lee *et al*. 2008). None of these stains, however, can be used when cassava microspores have an intact exine. The combination of CLSM analysis and microspore samples with partially digested exine, as optimized and used in this study, proved to be useful not only for the identification of microspore stage of development but also for the confirmation of androgenesis induction. Similar applications may be useful to other species with thick-exine microspores such as rubber tree and coffee.

Cassava is an important crop in the tropics and this article contributes with basic information that will hopefully allow the application of different technologies for the genetic improvement of this crop.

References

Alves, C.A.A.: Cassava botany and physiology. - In: Hillocks, R.J., Tresh J.M., Bellotti A.C. (ed.): Cassava: Biology, Production and Utilization. Pp. 67-89. CABI Publishing, London 2002.

Barinova, J., Zhexembekova, M., Barsova, E., Lukyanov, S., Heberle-Bors, E., Touraev, A.: *Anthirinum majus* mircospore maturation and transient transformation *in vitro*. - J. exp. Bot. **53**: 1119-1129, 2002.

Berry, P.E., Cordeiro, I., Wiedenhoeft, A.C., Vitorino-Cruz, M.A., Ribes de Lima, L.: Brasiliocroton, a new crotonoid genus of *Euhphorbiacea* from Eastern Brazil. – Syst. Bot. **30**: 357-365, 2005.

Blackmore, S., Wortley, A.H., Skvarla, J.J., Rowley, J.R.: Pollen wall development in flowering plants. - New Phytol. **174**: 483-498, 2007.

Boavida, L.C., Becker J.D., Feijó J.A.: The making of gametes in higher plants. - Int. J. dev. Biol. **49**: 595-614, 2005.

Ceballos, H., Fregene, M., Pérez, J.C., Morante, N, Calle, F.: Cassava genetic improvement. - In: Kang, M.S., Priyadarshan P.M. (ed.) Breeding Major Food Staples. Pp. 365-391, Blackwell Publishing, Ames 2007.

Ceballos, H., Iglesias, C.A., Pérez J.C., Dixon A.G.O.: Cassava breeding: opportunities. - Plant mol. Biol. **56**: 503-515, 2004.

Chen, C.B., Xu, Y.Y., Ma, H., Chong, K.: Cell biological characterization of male meiosis and pollen development in rice. - J. Integr. Plant Biol. **47**: 734-744, 2005.

Custódio, L., Carneiro, M.F., Romano, A.: Microsporogenesis and anther culture in carob tree (*Ceratonia siliqua* L.). - Sci. Hort.**104**: 65-77, 2005.

Da Silva, R.M., Bandel, G., Faraldo, M.I.F., Martins, P.S.: Biología reprodutiva de etnovariedades de mandioca. - Sci. Agr. **58**: 101-107, 2001. [In Span.]

De Carvalho, R.D., Guerra, M.: Cytogenetics of *Manihot esculenta* Crantz (cassava) and eight related species. - Hereditas **136**: 159-168, 2002.

De Souza, M.M., Pereira, T.N.S.: Development of pollen grain in yellow passion-fruit (*Passiflora edulis* f. *flavicarpa*; *Passifloraceae*). - Genet. mol. Biol. **23**: 469-473, 2000.

Esau, K.: Anatomy of Seed Plants. - Wiley, New York 1977.

Fan, Z., Armstrong, K.C., Keller, W.A.: Development of microspores *in vivo* and *in vitro* in *Brassica napus* L. - Protoplasma **147**: 191-199, 1988.

Goldberg, R.B., Beals, T.P., Sanders, P.M.: Anther development: basic principles and practical applications. - Plant Cell **5**: 1217-1229, 1993.

Halsey, M.E., Olsen, K.M., Taylor, N.J., Chavarriaga-Aguirre, P.: Reproductive biology of cassava (*Manihot escultenta* Crantz) and isolation of experimental field trials. - Crop Sci. **48**: 49-58, 2008.

Heslop-Harrison, J.: Cytoplasm connections between angiosperm meiocytes. - Ann. Bot. **30**: 221-230, 1966.

Hrabina, M., Jain, K., Gouyon, B.: Cross-reactivity between pollen allergens from common *Pooideae* grasses and cultivated cereals. - Clin. exp. Allergy Rev. **8**: 18-20, 2008.

Huang, B., Bird, S., Kemble, R., Simmonds, D., Keller, W., Miki, B.: Effects of culture density, conditioned medium and feeder cultures on microspore embryogenesis in *Brassica napus* L. cv. Topas. - Plant Cell Rep. **8**: 594-597, 1990.

Jennings, D.L.: Variation in pollen and ovule fertility in varieties of cassava, and the effect of interspecific crossing on fertility. - Euphytica **12**: 69-76, 1963.

Kasperbauer, M.J., Wilson, H.M:. Haploid plant production and use. - USDA Technol. Bull. **1586**: 33-39, 1979.

Kernan, Z., Ferrie, A.M.R.: Microspore embryogenesis and the development of a double haploidy protocol for cow cockle (*Saponaria vaccaria*). - Plant Cell Rep. **25**: 274-280, 2006.

Khan, F.A., Ahmad, S., Siddiqui, S.A.: Microsporogenesis and development of male gametophyte in some *Solanum* species. - Beitr. Biol. Pflanz. **66**: 1-7, 1991.

Kindiger, B., Beckett, J.B.: A hematoxilin staining procedure for maize pollen grain chromosomes. - Stain Technol. **60**: 265-269, 1985.

Koltunow, A.M., Truettner, J., Cox, K.H., Wallroth, M., Goldberg, R.B.: Different temporal and spatial gene expression. - Plant Cell **2**: 1201-1224, 1990.

Koti, S., Reddy, K.R., Kakani, V.G., Zhao, D., Reddy, V.R.: Soybean (*Glycine max*) pollen germination characteristics, flower and pollen morphology in response to enhanced ultraviolet-B radiation. - Ann. Bot. **94**: 855-864, 2004.

Lauxen, M.S., Kaltchuk-Santos, E., Hu, C., Callegari-Jacquesi, S.M., Bodanese-Zanettini, M.H.: Association between floral bud size and developmental stage in soybean microspores. - Braz. Arch. Biol. Technol. **46**: 515-520, 2003.

Lee, Y., Kim, E.S., Choi,Y. Hwang, I., Staiger, J., Chung, Y.Y., Lee, Y.: The *Arabidopsis* phosphatildylinositol-3-kinase is important for pollen development. - Plant Physiol. **147**: 1886-1897, 2008.

Li, D.X., Lin, M.Z., Wang, Y.Y., Tian, H.Q.: Synergid: a key link in fertilization of angiosperms. - Biol. Plant. **53**: 401-407, 2009.

Liu, W., Zheng, M.Y., Polle, E.A., Konzak, C.F.: Highly efficient doubled-haploid production in wheat (*Triticum aestivum* L.) via induced microspore embryogenesis. - Crop Sci. **42**: 686-692, 2002.

Mariani, C., Beuckeleer, M.D., Truettner, J., Leemans, J., Goldberg, R.B.: Induction of male sterility in plants by a chimaric ribonuclease gene. - Nature **347**: 737-741, 1990.

Mascarenhas J.P.: The biochemistry of angiosperm pollen development. - Bot. Rev. **41**: 259-314, 1975.

McCormick, S.: Control of male gametophyte development. - Plant Cell **16**(Suppl.): S142-S153, 2004.

Nowack, M.K., Grini, P.E., Jakoby, M.J., Lafos, M., Koncz, C., Schnittger, A.: A positive signal from the fertilization of the egg cell sets off endosperm proliferation in angiosperm embryogenesis. - Nat. Genet. **38**: 63-67, 2006.

Ospina, B., Ceballos, H.: La yuca en el tercer milenio.[Cassava in the Third Milenium.] - CIAT Publication, Cali 2002. [In Span.]

Owen, H.A., Makaroff, C.A.: Ultrastructure of microsporogenesis and microgametogenesis in *Arabidopsis thaliana*

(L.) Heynh. ecotype Wassilewskija (*Brassicaceae*). - Protoplasma **185**: 7-21, 1995.

Ressayre, A., Raquin, C., Mignot, A., Godelle, B, Gouyon, P.H.: Correlated variation in microtubule distribution, callose deposition during male post-meiotic cytokinesis, and pollen aperture number across *Nicotiana* species (*Solanaceae*). - Amer. J.Bot. **89**: 393-400, 2002.

Reynolds, E.S.: The use of lead citrate at high pH as an electron-opaque stain for electron microscopy. - J. cell. Biol. **17**: 208-213, 1963.

Rowley, J.R., Claugher, D., Skvarla, J.J.: Structure of the exine in *Artemisia vulgaris* (*Asteraceae*): a review. - Taiwania **44**: 1-21, 1999.

Scott, R.J., Spielman, M., Dickinson, H.G.: Stamen structure and function. - Plant Cell **16**(Suppl.): S46-S60, 2004.

Scott, R., Hodge, R., Paul, W., Draper, J.: The molecular biology of anther differentiation. - Plant Sci. **80**: 167-191, 1991.

Summers, W.L., Jaramillo, J., Bailey, T.: Microspore developmental stage and anther length influence the induction of tomato anther callus. - HortScience **27**: 838-840, 1992.

Taskin, K.M., Turgut, K. Scott, R.J.: Apomeiotic pollen mother cell development in the apomictic *Boechera* species. – Biol. Plant. **53**: 468-474, 2009.

Tomasi, P., Dierig, D.A., Backhaus, R.A., Pigg, K.B.: Floral bud and mean petal length as morphological predictors of microspore cytological stage in Lesquerella. - HortScience **34**: 1269-1270, 1999.

Widholm, J.M.: The use of fluorescein diacetate and phenolsaphranine for determining viability of the cultured plant cells.- Stain Technol. **47**: 189-194, 1972.